

A Gel Lung-Equivalent Material for 3D Dosimetry



**Joao A. Borges^{a)}, M.S., José A. Bencomo, Ph.D.¹⁾, Geoffrey S. Ibbott, Ph.D.²⁾,
and Jingfei Ma, Ph.D.³⁾**

**a), 1), 2) Departments of Radiation Physics, ³⁾ Department of Imaging Physics
University of Texas-M.D. Anderson Cancer Center
1515 Holcombe Blvd, Houston, Texas 77030-4009**

This work was supported by National Research Council and the IAEA Fellowship BRA/02022R, and PHS grant CA 10953 awarded by the NCI, DHHS.

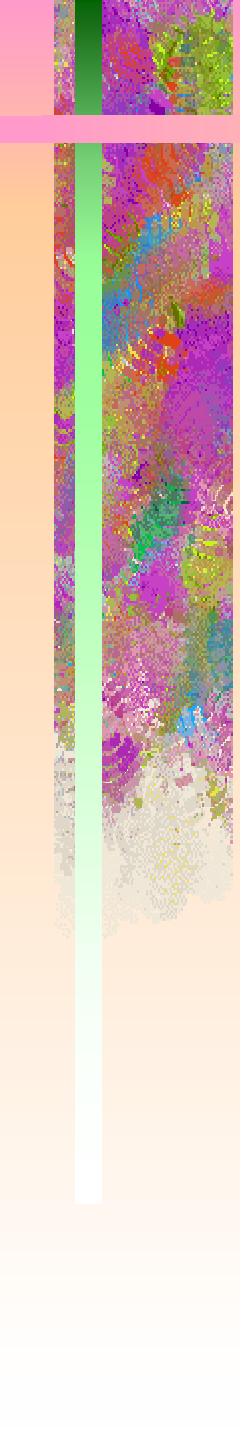
Abstract

Quality assurance of treatment delivery with advance radiotherapy technology is difficult, especially in inhomogeneous media, because the lack of electronic equilibrium. The purpose of this study was to evaluate a polymer-gel-dosimeter (PGD) for 3D verification of dose distributions in lung. The PGD to be used is MAGIC gel. To achieve a lung density PGD, an Erlenmeyer flask was filled to the top with styrofoam beads, flushed with nitrogen to remove any oxygen inside the flask and beads. The gel was then infused into the flask. The PGD was irradiated with a 16 cm² field to 5 Gy in the 6 MV photon beam of a Clinac 2100C Linac, along to central axis of the flask. The PGD was then scanned on a 1.5 Tesla MRI scanner before and after irradiation, using a multiple spin-echo sequence (TE/TR/Pixel Size = 20-640ms/4s/1mm). Least-square fitting the pixel values from 32 consecutive images using a single exponential decay function derived the R2 relaxation rates. Subtracting pixel values of pre and post-irradiated images eliminated artifacts. Depth-dose-data (PDD) were generated from the R2 images and compared to PDD generated by EGSnrc Monte Carlo simulation (MCS). MCS was performed using low-density water as material. Preliminary results show good agreement between depth dose measured with the PGD and the depth dose calculated using MCS. The PGD will be use to evaluate 3D-treatments plans in a breast anthropomorphic phantom.

Introduction

The increasing complexity of treatment planning and radiation dose delivery systems particularly for conformal and intensity modulated radiotherapy has required a concomitant increase in the sophistication of treatment verification technology. Consequently, there has been an increased interest in the development of 3D radiation dose measuring devices. Gel dosimeters have proven to be reliable and precise radiation detectors to measure dose distributions in three dimensions. Recent developments in Gel dosimeters have allowed evaluating the accuracy of patient's treatments with complex field shapes and large dose gradients as delivered by advanced technology radiation delivery systems (McJury *et al*/2000).

Gel dosimeters are tissue equivalent materials and are made of water, gelatin, and acrylic monomers (polymer gels). Gel dosimetry is based in the degree of polymerization of monomers produced by the water hydrolysis induce by radiation. The degree of polymerization depends on the initial amount of free radicals generated by the radiation dose (McJury *et al*/2000).



Introduction (1)

Gel dosimeters are tissue equivalent materials and are made of water, gelatin, and acrylic monomers (polymer gels). Gel dosimetry is based in the degree of polymerization of monomers produced by the water hydrolysis induce by radiation. The degree of polymerization depends on the initial amount of free radicals generated by the radiation dose (McJury *et al*/2000).

MRI, x-ray and optical CT have been used to study the degree of polymerization induce by radiation. In the x-ray and optical CT techniques the bean attenuation through the Gel is related to the polymer density, and indirectly to the radiation dose delivered to the Gel. In the MRI technique, the water transverse relaxation rate R2 (reciprocal of the transverse relaxation time T2) is linearly related to dose between 0 and 50 Gy, This relationship is due to the alteration produced by radiation of the binding states of water molecules to the Gel polymer lattice.

Introduction (2)

Gel dosimeters are excellent radiation detector devices for the evaluation of dose absorbed in homogeneous media, where there is electronic equilibrium. In contrast, there are no reports in the literature of radiation dosimeters able to accurately evaluate 3D-dose distributions in a non-homogeneous media such as the breast and lungs tissues. Olberg *et al* (2000) attempted to make a lung equivalent dosimeter using Fricke gel (ref), However, this gel dosimeter is denser than the lung tissue, it is very difficult to prepare, and difficult to use inside of an anthropomorphic phantom.

The purpose of this thesis is to develop a low-density polymer gel, using a mixture of Styrofoam beads and a polymer Gel dosimeter. This new dosimeter will be use to measure 3D-dose distributions inside a non-homogeneous media such as lung tissue.

Materials Methods- *Lung model*

In humans, approximately 10% of the lung is occupied by solid tissue, whereas the remainder is filled with air and blood. Gas exchange occurs in approximately 300 million of alveolus. The alveolus is a thin walled polyhedral sack, it is reasonable to assume that the lung is made of millions of air beads in a water volume as shown in **figure 1**. Therefore, a lattice of cubic cells will be used to represent the bead distribution in this lung model. **Figure 2**. Shows that the frontal cube's face includes a bead's central cut of diameter d centered on the face, and four quarter bead' central cuts each centered on each one of the apices of the cube

Fig. 1

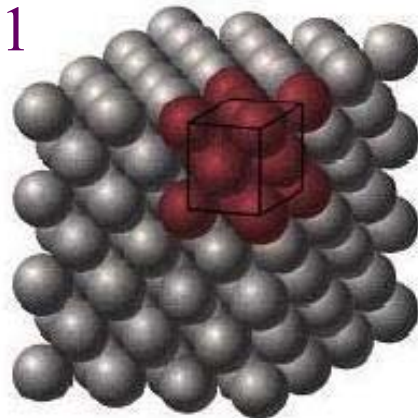
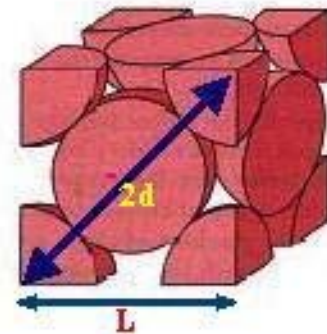


Fig. 2



Materials Methods- *Lung model (1)*

The relationship between the side L of a cube and the diameter d of a bead is $(2d)^2 = L^2 + L^2$, the bead volume (internal volume of the cubic cell occupied by the bead) is $4 \times \frac{4}{3} \pi \left(\frac{d}{2}\right)^3$ and the cubic cell volume is L^3 . So, the ratio between the bead volume and cubic cell volume is 0.74.

It gives us a cell density that dependent of bead density and interstitial material density , independent of bead diameter. The cell density is given by:

$$\rho_{cell} = 0.74 \rho_{be} + 0.26 \rho_{int}$$

Materials Methods- *Lung model (2)*

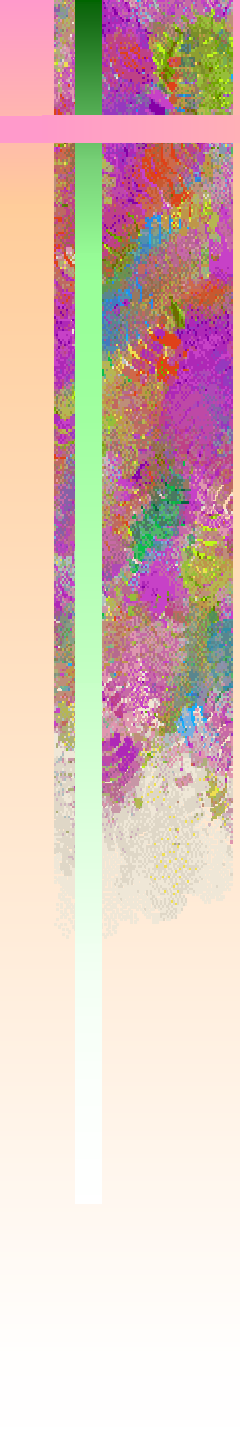
The Styrofoam bead's density is approximately 0.003 g/cm³ and the polymer Gel density that is used our lung model is approximately 1.060 g/cm³, then the Styrofoam-polymer Gel mixture has a density of 0.27782 g/cm³.

This density is very close to the lung density of approximately 0.3 g /cm³.

Gel preparation

The Gel was manufactured under normal atmospheric conditions using the formulation proposed by Fong *et al* (2001), which is: 8% gelatin by weight (300 bloom Aldrich; Milwaukee, WI), 9% methacrylic acid by weight (Sigma; St Louis, MO), ascorbic acid (2×10^{-3} M, Mallinkrodt; Paris, KY), $\text{CuSO}_4 \cdot 5\text{H}_2\text{O}$ (8×10^{-5} M, Aldrich; Milwaukee, WI), hydroquinone (1.8×10^{-2} M, Sigma; St Louis, MO) and de-ionized water, This Gel formula is known as MAGIC Gel.

To prepare a batch of one-liter of Gel, the following process has to be followed: It began by placing 714 ml of water and 80g of gelatin in a glass flask with a stir-bar inside.



Gel preparation (1)

Then the flask is put above an electrical plate with magnetic stirring and heated to 50°C, after the gelatin is completely dissolved, 2g of hydroquinone in 48 ml of de-ionized water are added the solution, the solution is then allow to cool. When the solution is cooled to approximately 37°C. 0.353g of ascorbic acid is diluted in 50 ml of de-ionized water, 0.02g of $\text{CuSO}_4 \cdot 5\text{H}_2\text{O}$ are diluted in 30 ml of de-ionized water and finally 90g of methacrylic acid are added to the flask. Before using the Gel, it is heated to 40°C.

The Gel is injected in cylindrical containers constructed of Barex (BP Chemical, London). Barex is chosen because it has less permeability for oxygen and is easily thermoformed. The dimensions of each container are 8 cm height by 10 cm diameter. Each container has a polystyrene top with 2 holes. Rubber stopper were used to seal the containers



Gel preparation (2)

Two Barex containers were filled each with a different bead diameter, and a third container was filled only with Gel. The small beads diameter is approximately 1 mm and the large beads diameter is approximately 3mm. After all the containers were sealed, those containers filled with beads were flushed with nitrogen to remove any oxygen inside, 24hours before injecting the Gel. To allow the nitrogen to flow out when injecting the Gel three needles were placed through the stoppers, one needle connected to the nitrogen dispenser, another was use to inject the Gel and the third one was used to ventilate to the atmosphere.

Gel preparation (3)

The **figures 3** shows two Gel containers one filled with small beads and the other with large beads. **Figure 4** shows the setup to flush the containers.



Fig. 3



Fig. 4

Gel Irradiation

Each Gel container was irradiated to 10 Gy at room temperature using a 4 x 4 cm² square field and a 6 MV photon beam from a Clinac 2100C machine, 24 hours after the preparation of the Gel. Each container was irradiated upside down inside of a 30cmx30cmx30cm water tank. To insure a maximum dose at the surface of the container, water was added to form a 1.5 cm layer above the surface of the container.

See figure 5.



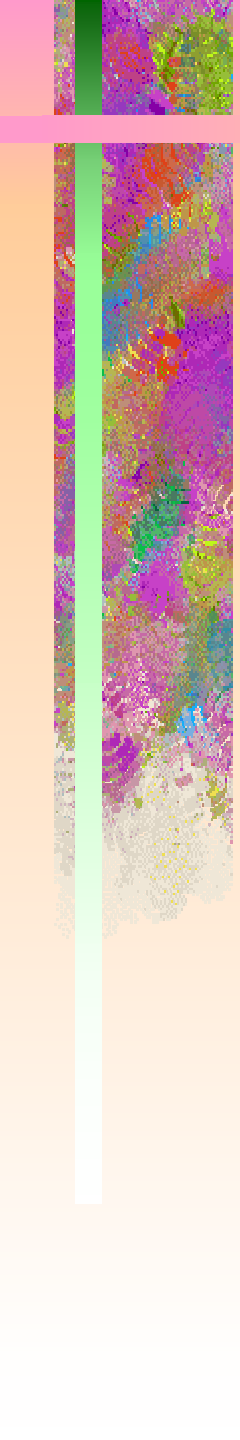
Fig. 5

MR imaging and processing

After Irradiation the containers were scanned inside an RF head coil using a 1.5T GE MRI machine. Four spin-echo sequences were used, each one with different echo time's intervals and a TR of 4s. The echo time intervals were 20, 35, 100 and 250 ms, each scan produced four images. This scanning protocol produces a set of four images per plane each one obtained as follows: the first one at 20, 40, 60 and 80 ms; the second one at 35, 70, 105 and 140 ms; the third one at 100, 200, 300 and 400 ms; and last one at 250, 500, 750 and 1000 ms. The containers were scanned at mid-sagittal plane. The images were acquired in a 256 x 256 matrix with a field size of 32 x 32 cm² and slice thickness of 5 mm. The gain set of the machine was equal in all acquisitions. **Figure 6** shows the setup used to scan the containers.



Fig. 6



MR imaging and processing

To obtain the transverse relaxation rate values, the pixels values of a set of MR images all obtained at same position were fitted to a single exponential function given by:

$$y(t) = A \times \exp(t_0 - R2 \times t) + B$$

Where A, B and t_0 are constants, t is the time and R2 the transverse relaxation rate. The exponential functions of each set are link by A, B and R2 values during the fitting; the four functions should have the same values. The other constant t_0 was not linked during the process of improving the fitting quality, as the images belong to different sets. The image processing was accomplished using the Interactive Data Language (IDL, Research Systems, Boulder, CO, USA).

Curve profiles were taken of the mid-sagittal plane R2 images generated after the fitting. The profile along the mid-sagittal plane of the container without beads was compared to Percent Depth-dose curves of the machine and Monte Carlo (MC) simulation; the containers with beads were compared only to MC simulation. To compare the curves they were normalized to their areas (the area used was between the maximum and 5.5 cm depth) then they were normalized to 100%.

Monte Carlo

To generate the Percentage Depth-Dose curves for the 6 MV photon beam attenuation through the lung Gel and the soft tissue Gel a Monte Carlo simulation was performed using the EGSnrc code (Kawrakow and Rogers) and the DOSRZ code was used to define the geometry in the calculations. The geometrical model was defined as a cylindrical volume of 8-cm height and 10 cm diameter and a polystyrene top of 3-cm height. The cylinder was placed along the beam axis and at 1.5-cm depth in semi-infinite water phantom. The materials simulated inside the cylindrical volume were water of normal density to simulate the tissue equivalent Gel and low-density water (0.28 g/cm^3) to simulate the lung equivalent Gel. The volume of the cylindrical containers was divided in small cylinders of 0.125-cm thick by 1-cm diameter all arranged with their central axis parallel to the photon beam central axis. This procedure was used by the MC code to calculate the dose inside the containers.

Monte Carlo (1)

The source was simulated in the MC code by a point source of photons located at 100 cm from the surface of a semi-infinite water phantom. The photons beam is perpendicularly incident on the surface of the phantom. In the MC simulation the 6 MV beam X-rays spectrum published by Mohan *et al* (1985) was used. The simulated field size has a circular diameter of 4.5 cm (the equivalent diameter of this field size is 4 cm square) at the surface of the phantom. The histories of 5×10^6 photons were followed. The simulation was carried out using an energy threshold of 0.521 MeV for the electrons and 0.01 MeV for the photon. The EGSnrc code provided the interaction cross-section data for water.



Gel density

To verify the lung-Gel density a CT scan of the containers filled with Styrofoam beads was performed. A total of 20 images were taken of the mid-sagittal plane of the lung-Gel, and the average CT number from the 20 images was compared to the CT number obtained from the calibration curve of the CT scanner.

Results-*MR images*

Figure 7 show four rows of images, each row represents one MRI scan of the Gel made with small beads. The four images in the first row were obtained using a TE interval of 20 ms. The images in the second row were obtained with a TE interval of 35 ms. The images in the third row were obtained with a TE interval of 100 ms. Finally, the images in the fourth row were obtained with a TE interval of 250 ms.

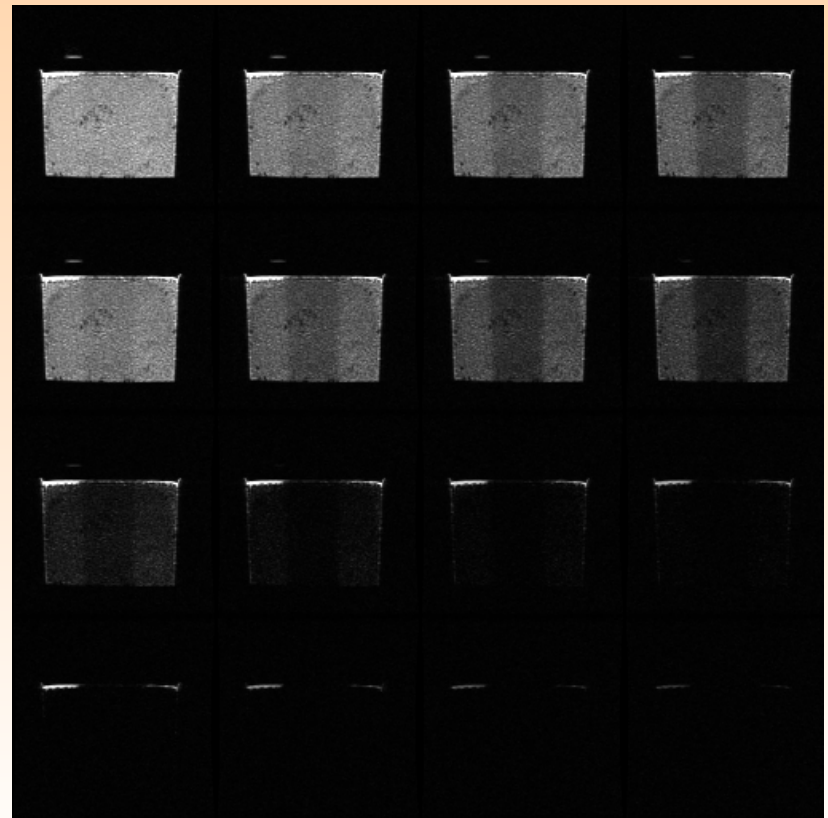
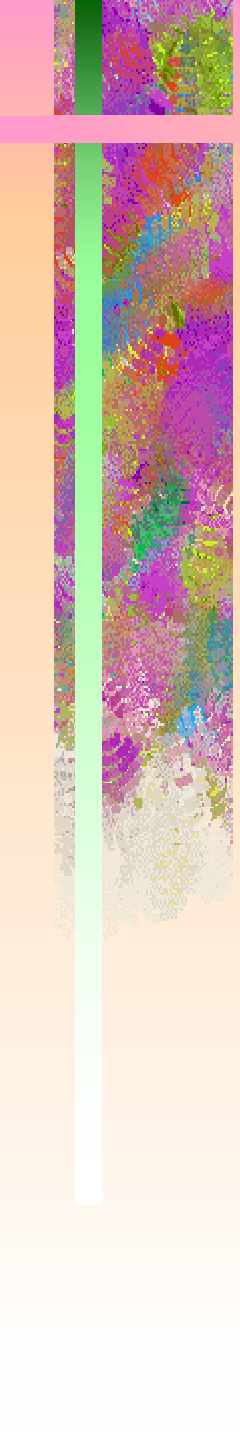


Fig. 7



Results-*MR images (1)*

For each row of images in **figure 7**, the regions of low signal intensity in the middle of each image represents the region irradiated with 6 MV photons. In reference to the first row in **figure 7**, it can be observed from left to right that the signal intensity from the irradiated region decreases faster than the signal from the non-irradiated region. This change in signal intensity result from a larger value of $R2$ for the irradiated region than the $R2$ value for the non-irradiated region. The Gel has a higher density at the top of the container because it is very difficult to mix the gel with the beads in this region. This higher density produces larger signal intensity at the top of each image as can be seen on **figure 7**.

R2 images map

Figure 8 shows the R2 maps of (a) the high-density Gel, (b) the Gel mixed with small beads, and (c) the Gel mixed with big beads. The R2 difference between the irradiated and non-irradiated regions of the Gel is higher in the container with the high-density Gel (a). As seen in Figure 8 (a) R2 varies along the longitudinal axis of the container; this results from the photon beam attenuation by the high-density Gel. The lines on the images a, b, and c delimit the region where profiles were obtained.

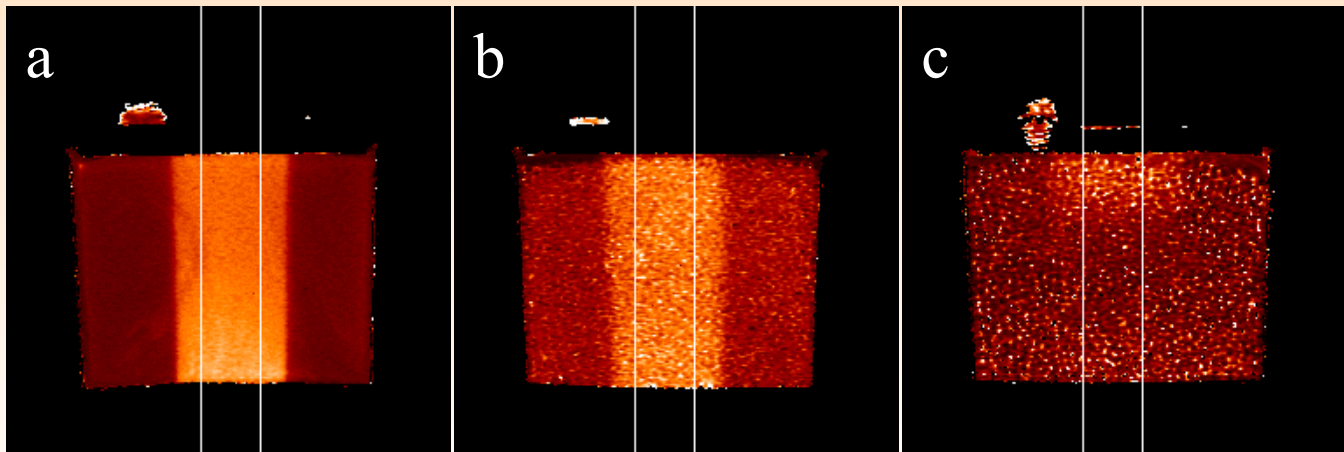


Fig. 8



R2 images map (1)

The Gel mixed with small bead show a small but visible difference in R2 between the irradiated and non-irradiated regions of the Gel. However, the effect of beam attenuation along the axis of the container is not very obvious as in the high-density Gel, This is due to the low beam attenuation by the low-density Gel.

The Gel mixed with big bead show a very small difference between the irradiated and non-irradiated regions of the Gel. Also notice the unexpected artifact in the top region of the image.



Curves

The curves in **figure 9** were obtained from the pixel value at the center of the irradiated region of the Gel for different echo-times. **Figure 9 (a)** shows the curve for the high-density Gel without beads and **figure 9 (b)** shows the curve for the Gel mixed with small beads. Both curves show discontinuities with the set of echo-time intervals. As seen in **figure 9** the most important discontinuity is between set of echo-time intervals of 35 ms and 100 ms. This discontinuities are due to the parameter t_0 which was allow to vary freely among echo-time intervals during the mathematical curve fitting. Another important source of discontinuity is that signal intensity of the Gel mixed with small beads is much lower than one from the high-density Gel.

Curves (1)

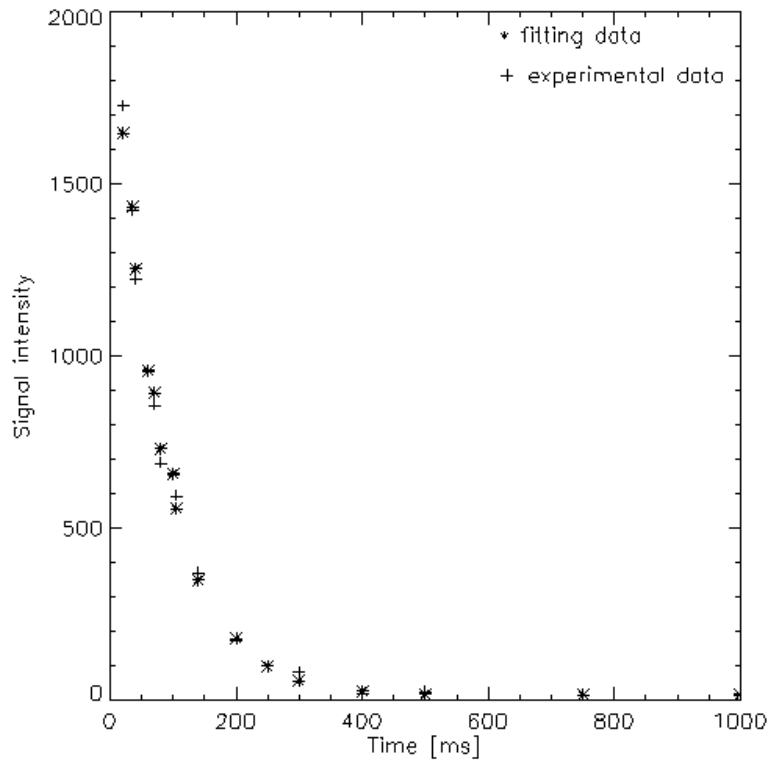


Fig. 9 a

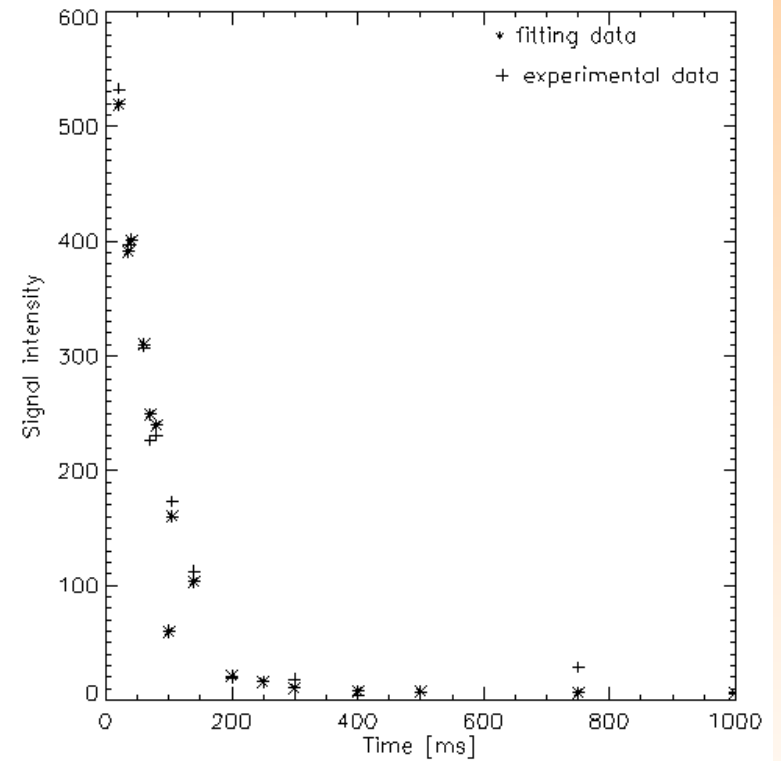
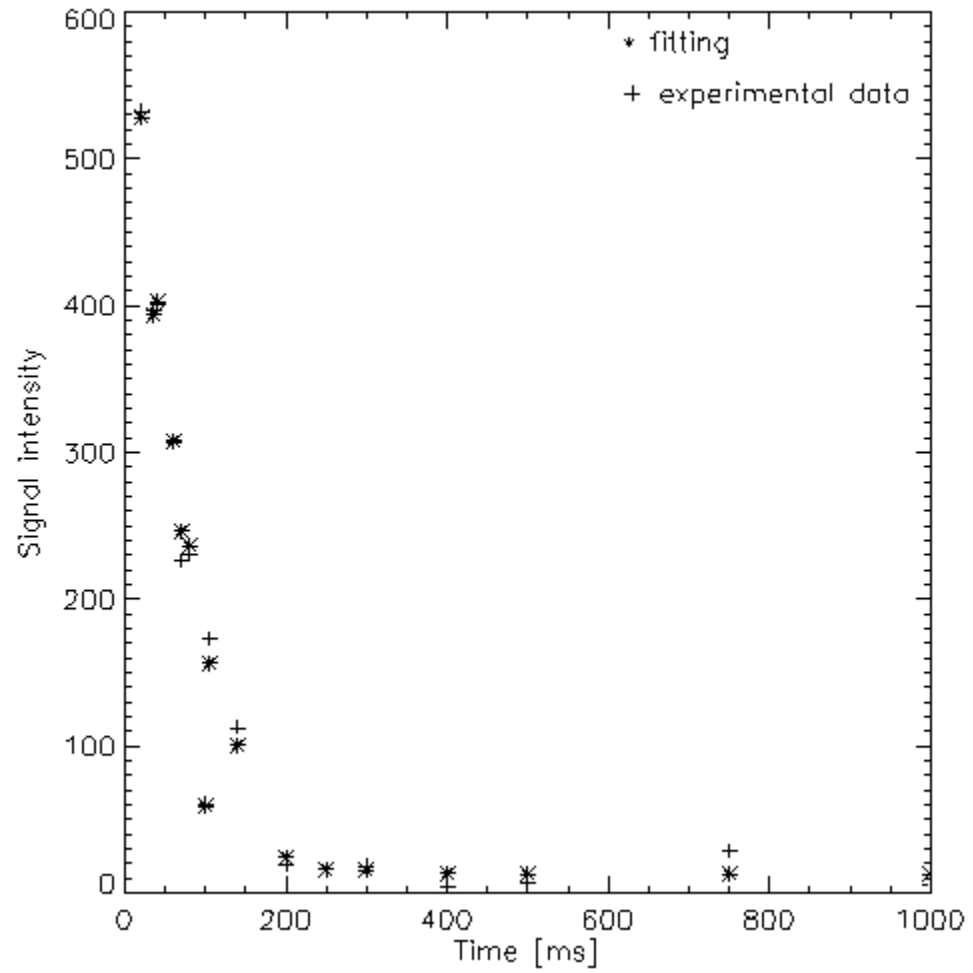


Fig. 9 b

Curves (2)

The profiles generated from the R2 images in figures 8a and 8b and also from figures 9a and 9b are plotted in figures 10a and 10b. The Percentage Depth dose curves (PDD) for the high-density Gel without beads and the Gel mixed with small beads are also plotted in figures 10a and 10b. The PDD for the 6 MV photon beam of the Clinac 2100C linear accelerator was obtained with a Wellhofer beam scanning system (model WP700 (v3.51.00) and Wellhofer IC04 ion chamber). In both figures 10a and 10b the firsts 1.5-cm correspond to the buildup region in water for the 6 MV photon beam. The data shown includes the data generated using Monte Carlo simulation. The region beyond the 1.5-cm depth is inside the Gel. Figures 10c and 10b show the difference between the experimental data (data from R2 maps) and the MC simulation of the high-density Gel without beads and the Gel mixed with small beads, receptively.





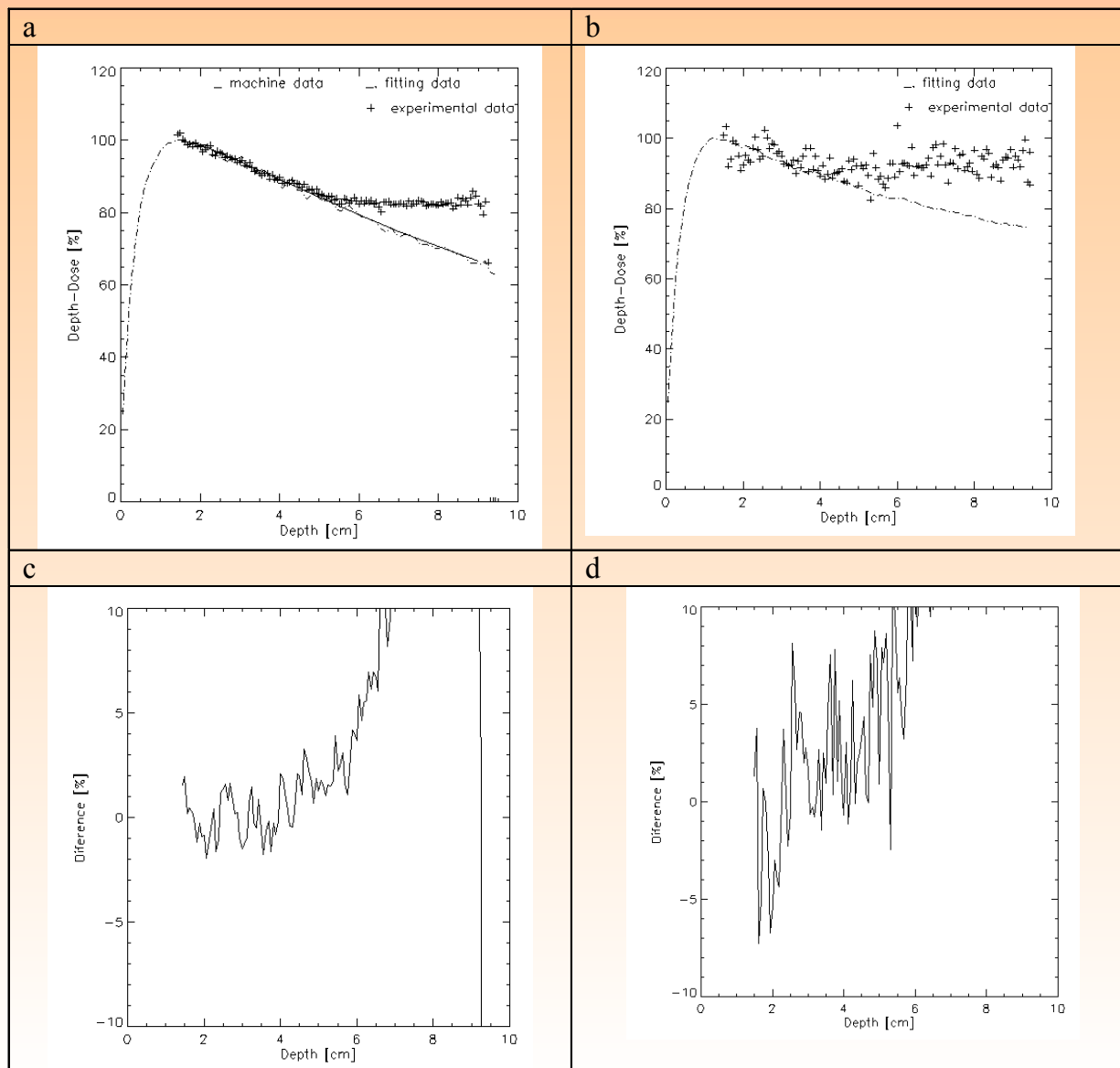
Curves (3)

In the high-density Gel without beads, figure 10a, the experimental data agree very well with the machine data and with the MC simulation up to approximately 4.5-cm depth. Experimental data for depths deeper than 4.5 cm show a plateau. The difference between the curves is smaller than $\pm 2.5\%$, up to approximately 4.5-cm depth then it increases quickly as shown in figure 10c. Figures 10a and 10 b also shows the excellent agreement between the data from MC simulation and the machine data.

The experimental data for the Gel mixed with small bead show the same behavior as the high-density Gel data. However the difference between the curves in figure 10b is larger, varying between $\pm 5.0\%$ up to 4.0-cm depth and then increases rapidly.

The curves for the Gel mixed with big beads are not shown because data are very noisy and completely disagree with the MC simulation

Figure 10.





CT number

The density of the Gel mixed with small beads was measured using CT images acquired with a Phillips.... CT scanned. Measurements show that it varies from 0.31 g/cm³ to 0.35 g/cm³. Use of scanner calibration?



Discussion and conclusion

The R2 maps suggest that the Gel mixed with small beads is less radiation sensitivity than the high-density Gel. This finding differs from one reported by Olberg *et al* (2000). In Olberg *et al* publication the lung gel equivalent material designed for their study showed higher radiation sensitivity than the pure gel.

The great difference between R2 maps of the Gel mixed with small beads and the Gel mixed with big beads suggest a dependence of R2 value on the bead size, probably due a lack of radiation equilibrium in the Gel mixed with big beads. To study such effect, future work will include an MC simulation using the lattice of cubic cells in [figure 2](#).

The curves in [figure 9](#) did not show the single exponential behavior expected from R2 measurements, particularly for the Gel mixed with beads. The discontinuities in the curves shown in [figures 9a and 9b](#) may be due to the use of different spin-echo sequences to acquire the data shown in those figures. Such acquisition protocol and the use of a head coil to perform the Gel scans may explain the bad agreement between experimental data and MC simulation for depths beyond 4.5 cm.



Discussion and conclusion (1)

Deene (2001) demonstrated that using of a head coil and a multi spin-echo sequence to acquire T2 weighted images of monomer-polymer gel dosimeters produce non-uniformities in the images. R2 maps of a homogeneous cylindrical Gel scanned using a head coil were found to be uniform only in center of the coil. Spin-echo sequences with non-equal echo time intervals also cause severe non-uniformities in the R2 maps. Deene concluded that using spin-echo sequences with equal echo-time intervals to measure the R2 distribution in the phantom before the irradiation and using this image as a template to correct the R2 maps generated after irradiation, he could improve the accuracy of the R2 maps.

In this study R2 maps acquired before the irradiation of the Gels were used to verify the R2 maps uniformity. The **figure 11** shows a profile of the R2 map of the Gel before irradiation. The profile shows non-uniformity in the same region (beyond 4.5-cm depth) the same region where the experimental data acquired in this study do not agree with the MC simulation or the machine data.

Discussion and conclusion(2)

That R2 map shown in figures 11 was not used as a correction template because the gain sets of the machine during the scan of the Gel before and after irradiation were different.

Deene (2001) also suggest the use of a body coil to scan the Gel, the problem with this approach is that the signal-to-noise ratio from the Gel will be significantly lower.

The use of an R2 maps acquisition protocols with a larger number of excitations may also improve the agreement between Gel data and the machine data or MC simulation, principally for the Gel mixed with small or big beads.

A future study using the above recommendations needs to be perform to verify the accuracy of the Gels with low-density when used for 3D dosimetry.

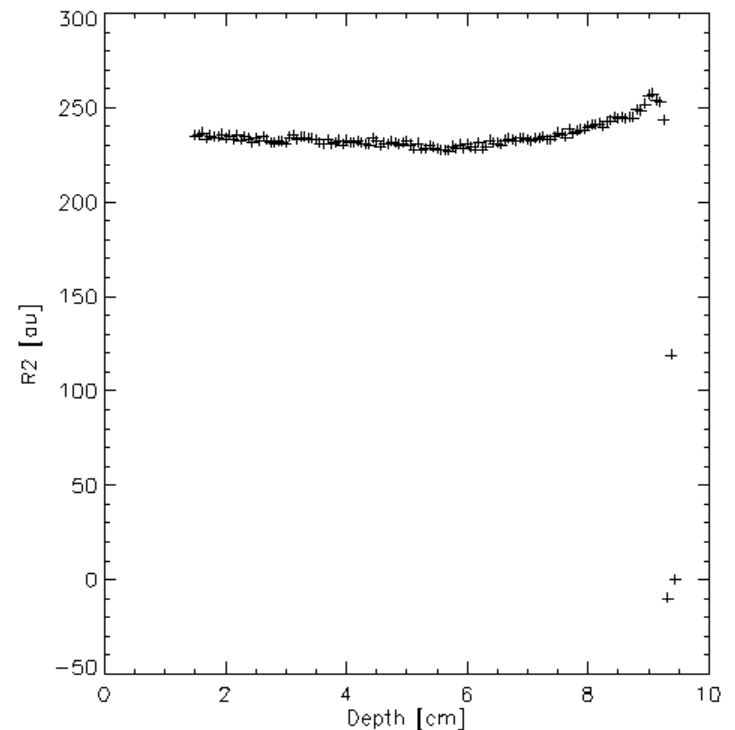


Figure 11.

References

1. Deene Y Fundamental of MRI measurements for gel dosimetry *Preliminary Proceedings of 2nd International Conference on Radiotherapy Gel Dosimetry*49-65
2. Fong P M, Keil D C, Does M D and Gore J C 2001 Polymer gel for magnetic resonance imaging of radiation dose distribution at normal room atmosphere *Phys. Med. Biol.* **46** 3105-3113
3. Kawrakow I and Rogers D W O The EGSnrc code system: Monte Carlo simulation of electron and photon transport *NRCC Report PIRS-701*
4. McJury A, Oldham M, Cosgrove V P, Murphy P S, Doran S, Oleach M O and Webb S 2000 Radiation dosimetry using polymer gels: methods and applications *The British Journal of Radiology* **73** 919-929
5. Moran R, Chui C and Lidofsky L Energy and angular distributions of photons from medical linear accelerators *Med. Phys.* **12** 592-597
6. Olberg S, Skretting A, Bruland O and Olsen R 2000 Dose distribution measurements by MRI of phantom containing lung tissue equivalent compartments made of ferrous sulfate gel *Phys. Med. Biol.* **45** 2761-2770

